Nuclei with diffuse surfaces for future Boltzmann-Uehling-Uhlenbeck calculations

S. J. Lee, H. H. Gan, E. D. Cooper, and S. Das Gupta
Physics Department, McGill University, Montreal, Quebec, Canada H3A 2T8
(Received 23 November 1987; revised manuscript received 16 June 1989)

The diffusivity of the nuclear surface plays an important role in peripherial collisions between two heavy ions. We show that a finite range force produces a diffuse surface for static nuclei in the Vlasov prescription. The surface is calculated self-consistently. This will allow us to perform more realistic calculations for peripheral reactions in the Boltzmann-Uehling-Uhlenbeck model.

I. INTRODUCTION

The Boltzmann-Uehling-Uhlenbeck (BUU) equations have become an important tool for theoretical analysis of heavy-ion collisions. Fluctuations can also be built into BUU,[1,2] so that one can now address the questions of multifragmentation, velocity distributions of spectator-like fragments, slowing down of spectators, and a host of detailed questions. The mean-field propagation is solved in the Vlasov prescription; collisions are treated as in the cascade model.

The starting point of all these calculations are two nuclei approaching each other with a given impact parameter. In time-dependent Hartree-Fock (TDHF), the nuclei are initially in their Hartree-Fock ground state. In BUU one does not start with wave functions; one starts with initial phase-space densities. The phase-space density of each nucleus should be so chosen that it respects the Pauli principle and gives the lowest energy. For an isolated nucleus this phase-space density should also be stationary in time. For many applications the mean field is taken to be $U(r)=A\rho(r)+B\rho^{\sigma}(r)$ where the parameters A, B, and σ are fixed from nuclear matter saturation density, binding energy, and compressibility. With this mean field in the Vlasov prescription, the ground-state phase-space densities of finite nuclei are sharp spheres in both configuration and momentum space. Thus in most BUU calculations[3-6] the nuclei are initially prepared with a constant density up to some radius R; similarly there is constant density in momentum space up to some radius p_F. In practice, for time propagation numerical calculations employ grids of sides 1–1.5 fm; this builds up some small diffusivity in practice.

Actual nuclei do not have sharp surfaces; quantum-mechanical variational calculations reproduce surfaces of nuclei which are quite realistic. Nonetheless for many applications of BUU, this is not an important deficiency, especially where one is concerned with near-central collisions of heavy-ion collisions, such as for flow angles,[7] transverse momenta,[8] or pion productions.[9] In Ref. 2, however, we looked at peripheral collisions in order to see how well BUU can describe spectator dynamics (see also Refs. 10 and 11). As suspected, the nuclear surface plays an important role for quantitative predictions. Although not obvious, it is possible that a better treatment of the surface is needed for calculation of multifragmentation processes as well. We have, therefore, attempted to obtain better surfaces for nuclei staying within the Vlasov prescription.

Let us emphasize that our objective is not just to obtain better surfaces for nuclei; we want to stay within the Vlasov prescription so that practical calculations for intermediate energy heavy-ion collisions, which is our objective, can be implemented. It is clear that quantum corrections to Vlasov prescription would provide better surfaces. We tried this route but concluded that practical calculations would not be feasible. Instead, we use a finite range force for the mean field which makes the static Vlasov self-consistent density fall to zero less abruptly. As shown by Siemens[12] previously, merely adding a finite range force does not generate a fully realistic surface. The curvature in the asymptotic region will not be correct. However, a realistic surface thickness (defined here as the distance over which the density falls from 90% to 10% of its maximum value) can be obtained while keeping the binding energy, saturation density, and compressibility of nuclear matter unchanged. The approach that we present here increases computer time for practical calculation by about a factor of 5; this is significant but well within our feasibility range. In a later paper, we will compare our calculations with specific experimental data.

Theoretical calculations from Grand Accélérateur National d'Ions Lourds[13] (GANIL) do have a diffuse surface. There the phase-space density is mapped out by Gaussians whose width is chosen to fit the experimental surfaces. The centers of the Gaussians are chosen self-consistently. The objective in that work is to mock up some quantal behavior. Our approach here is different. The only quantum effect we keep is the Pauli principle in its classical limit. The rest is determined by the stationary solution of the Vlasov equation which is completely classical.

II. PROCEDURE FOR OBTAINING SELF-CONSISTENT SOLUTIONS

The Vlasov equation is

$$\frac{\partial f}{\partial t}+\frac{\mathbf{p}}{m}\cdot\nabla_r f-\nabla_r U\cdot\nabla_p f=0\ . \tag{1}$$

We require, as a starting point, for each individual nu-

cleus that will collide, an initialization that keeps $\partial f/\partial t=0$. We can prove directly that if $f(\mathbf{r},\mathbf{p})=f(H)$ where $H=(p^2/2m)+U(\mathbf{r})$ then we satisfy

$$\frac{\mathbf{p}}{m}\cdot\nabla_r f=\nabla_r U\cdot\nabla_p f \tag{2}$$

and hence $\partial f/\partial t=0$; U is, however, not an external potential. In the simplified problem that we will tackle here, U is generated by a

$$\rho(\mathbf{r})=\int f(\mathbf{r},\mathbf{p})d^3p \ .$$

We guess a value of $\rho(\mathbf{r})$ which then generates a $U(\mathbf{r})$ which then generates a $f(\mathbf{r},\mathbf{p})$ which must then generate the same $\rho(\mathbf{r})$ with which we started. Thus there is a self-consistency condition implied just as in Hartree-Fock. In the past, we have used

$$U(\mathbf{r})=A\rho(\mathbf{r})+B\rho^{\sigma}(\mathbf{r}) \ . \tag{3}$$

The potential-energy density for such a mean field is

$$V[\rho(\mathbf{r})]=\frac{A\rho^2(\mathbf{r})}{2}+\frac{B}{\sigma+1}\rho^{\sigma+1}(\mathbf{r}) \ . \tag{4}$$

The total energy for the system is

$$E=\int f(\mathbf{r},\mathbf{p})\frac{p^2}{2m}d^3p\,d^3r+\int V[\rho(\mathbf{r})]d^3r \ . \tag{5}$$

The phase-space density we choose must not violate the Pauli principle. The number of quantum states in a region of phase space $d^3r\,d^3p$ is $(4/h^3)d^3r\,d^3p$, where 4 accounts for spin-isospin degeneracy. Thus for N particles we can consider a distribution

$$f(\mathbf{r},\mathbf{p})=\frac{4}{h^3} \quad \text{for } r\le R \text{ and } p\le p_F$$
$$=0 \quad \text{otherwise} \ , \tag{6}$$

where

$$\frac{4\left[\frac{4\pi}{3}\right]^2R^3p_F^3}{h^3}=N \ . \tag{7}$$

This distribution has a uniform density $\rho=N/(4\pi R^3/3)$ and an energy per particle

$$\frac{E}{N}=\frac{3}{5}\frac{h^2}{2m}\left[\frac{3}{16\pi}\right]^{2/3}\rho^{2/3}+\frac{A}{2}\rho+\frac{B\rho^{\sigma}}{\sigma+1} \ . \tag{8}$$

We can minimize the right-hand side of Eq. (8) to find the optimum value of $\rho=\rho_0$. This fixes R. It is now easy to see that the following distribution is a minimum energy self-consistent solution:

$$f(\mathbf{r},\mathbf{p})=\frac{4}{h^3}\theta[\lambda-U(\mathbf{r})-p^2/2m] \ , \tag{9}$$

with

$$U(\mathbf{r})=U(\rho_0) \quad \text{for } r\le R$$
$$=0 \quad \text{for } r>R \ . \tag{10}$$

Here $\lambda=U(\rho_0)+p_F^2/2m$ and is negative. Equation (9) is of the form $f(\mathbf{r},\mathbf{p})=f(H)$; further the $U(\mathbf{r})$ of Eq. (10) generates an $f(\mathbf{r},\mathbf{p})$ [Eq. (9)] which generates a ρ which gives back the $U(\mathbf{r})$ we started from. By construction, it is also a minimum energy solution.

We now consider adding a finite range term to Eq. (3):

$$U(\mathbf{r})=A\rho(\mathbf{r})+B\rho^{\sigma}(\mathbf{r})+\int v(\mathbf{r},\mathbf{r}')\rho(\mathbf{r}')d^3r' \ . \tag{11}$$

The corresponding change in Eq. (4) is

$$V(\mathbf{r})=\frac{A\rho^2(\mathbf{r})}{2}+\frac{B}{\sigma+1}\rho^{\sigma+1}(\mathbf{r})+\frac{1}{2}\rho(\mathbf{r})\int v(\mathbf{r},\mathbf{r}')\rho(\mathbf{r}')d^3r' \ . \tag{12}$$

In this work we will take $v(\mathbf{r},\mathbf{r}')$ to be a Yukawa

$$v(\mathbf{r},\mathbf{r}')=V_0\frac{e^{-|\mathbf{r}-\mathbf{r}'|/a}}{|\mathbf{r}-\mathbf{r}'|/a}$$
$$=4\pi V_0\sum_{l,m}f_l(r,r',a)Y_{lm}(\theta,\phi)Y^*_{lm}(\theta',\phi') \ , \tag{13}$$

$$f_l(r,r',a)=i_l(r_<\!/a)k_l(r_>\!/a) \ , \tag{14}$$

where i_l,k_l are modified spherical Bessel functions. For spherically symmetric problems considered here, we will only need

$$i_0(x)=\frac{\sinh(x)}{x} \ , \tag{15}$$

$$k_0(x)=\frac{e^{-x}}{x} \ . \tag{16}$$

It is fairly obvious that, with a Yukawa term, the sharp surface in configuration space is no longer a self-consistent solution. Let us assume a sharp surface; the value of $U(\mathbf{r})$ near the edge will be different from that in the interior because of the finite range implied by Eq. (11). A different value of $U(\mathbf{r})$ will imply a different value of $\rho(\mathbf{r})$ [Eq. (9)]. Thus a numerical procedure will have to be developed when $v(\mathbf{r},\mathbf{r}')$ is finite range.

We use the following numerical method. Equation (9) gives

$$\frac{3h^3}{16\pi}\rho(r)=\{2m[\lambda-U(r)]\}^{3/2}\theta[\lambda-U(r)]$$

which we recast in the form

$$\left[\frac{3h^3}{16\pi}\rho(r)\right]^{2/3}+2m[A\rho(r)+B\rho^{\sigma}(r)]=2m[\lambda-U_y(r)] \ . \tag{17}$$

Here $U_y(r)$ is the contribution due to finite range Yukawa part. We now start with a guessed parametrized value of $\rho(r)$ such that $\int\rho(r)d^3r=N$ and proceed as follows.

(i) We compute $U_y(r)$.

(ii) We guess a value for λ; using known $U_y(r)$ and Eq. (17), we compute $\rho(r)$ from $r=0$ up to some r_0 where $\rho(r)$ goes to zero. This could, in principle, require extra care if the parameters of the force A, B, and σ are such that the left-hand side of Eq. (17) is not monotonic in the range of $\rho(r)$ that is relevant. However, the values of the

force parameters in the nuclear case are such (see Sec. IV) that this does not happen. If the left-hand side of Eq. (17) were not monotonic, one would get a discontinuity in $\rho(r)$ before $\rho(r)$ reaches the value zero.

(iii) We now check if $\int \rho(r) d^3r = N$; if not, the value of λ is altered and step (ii) is repeated until the required number of particles is obtained.

(iv) Steps (i)–(iii) are repeated until $\rho(r)$ calculated in two successive steps are identical to within a preassigned value. An adequate check is that the values of λ calculated in two successive iterations are the same within a prescribed value.

Figure 1 shows an example of the self-consistent $\rho(r)$ calculated with the following force parameters [Eq. (11)]: $A = -373.3$ MeV fm^3, $B = 3238.1$ MeV fm^6, $\sigma = 2$, and for the Yukawa $V_0 = -363$ MeV and range parameter $a = 0.459\,79$ fm. In Sec. IV, we will deal at length with choices of force parameters. In the same figure, we have also shown a density distribution using Myer's formula that we will regard as representing the experimental density distribution. This formula has been used in heavy-ion calculations before[14,15] and is given by

$$\rho(r) = \rho_0 \left[1 - \left[1 + \frac{R}{a} \right] \exp(-R/a) \frac{\sinh(r/a)}{r/a} \right], \quad r < R \ , \tag{18}$$

$$\rho(r) = \rho_0 \left[\frac{R}{a} \cosh(R/a) - \sinh(R/a) \right] \frac{e^{-r/a}}{r/a}, \quad r > R \ , \tag{19}$$

where $R = 1.18 A^{1/3}$ fm, $a = 1/\sqrt{2}$ fm. This distribution is sufficiently realistic for our purposes and has the advantage that equivalent sharp radius R is simply proportional to $A^{1/3}$, while the half-density radius of a Fermi distribution does not have this simple proportionality. The other advantage is that no special normalization is required to ensure that the total number of particles is correct, since

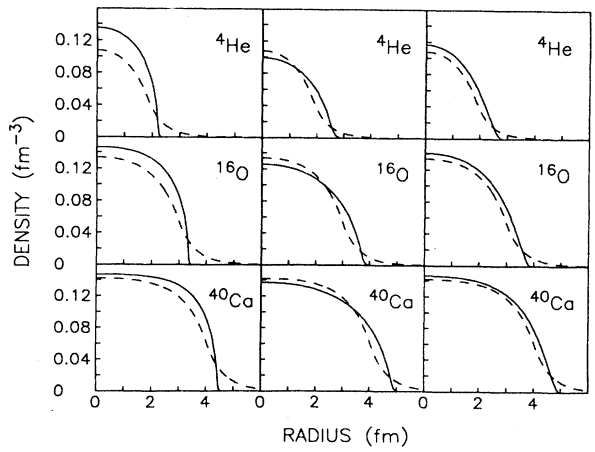

FIG. 1. Self-consistent nucleon density distributions (solid line) with stiff equation of state ($\sigma = 2$) compared to the Myers formula (dashed line). First column is with BKN force, second column with Eq. (30), and the last one with Eq. (29).

$$4\pi \int_0^\infty \rho(r) r^2 dr = \frac{4\pi}{3} \rho_0 R^3 \ ;$$

with this choice of R, $\rho_0 = 0.145$ fm^{-3}.

Figure 1 shows that the surface calculated in the Vlasov prescription is not diffuse enough. However, the diffusivity of the surface in our model is entirely determined by the parameters of the force used. In Sec. IV, we will choose parameters which produce more realistic surfaces. But, first, in the next section, we deal with some formal aspects of the Vlasov self-consistency condition. We show that finding a self-consistent solution is equivalent to finding an extremum of the energy. Further, a check can be made to test if the extremum is a minimum. This is analogous to Thouless theorem for the stability of a Hartree-Fock solution.[16,17]

III. SELF-CONSISTENCY, MINIMIZATION, AND STABILITY

We have $\rho(\mathbf{r}) = \int f(\mathbf{r},\mathbf{p}) d^3p$ and the potential energy depends only upon $\rho(\mathbf{r})$ but not upon $\mathbf{p}$. The kinetic-energy density is given by

$$T(\mathbf{r}) = \int d^3p \, f(\mathbf{r},\mathbf{p}) \frac{p^2}{2m} \ .$$

Since we are looking for minimum in energy, it makes sense to minimize the kinetic energy for a given $\rho(\mathbf{r})$. This is achieved by letting $f(\mathbf{r},\mathbf{p})$ be nonzero from $p = 0$ to some maximum $p_F(\mathbf{r})$. Thus we will have

$$f(\mathbf{r},\mathbf{p}) = \frac{4}{h^3} \theta[p_F(\mathbf{r}) - p] \ .$$

As before, the factor 4 takes into account spin-isospin and the condition $\tilde{f}^2 = \tilde{f}$, where $\tilde{f} = fh^3/4$, replaces the Hartree-Fock density-matrix condition $\rho^2 = \rho$.

The kinetic energy is

$$T = \int d^3r \, T(\mathbf{r}) = C \int \rho^{5/3}(\mathbf{r}) d^3r \ , \tag{20}$$

where

$$C = \frac{3h^2}{10m} \left[\frac{3}{16\pi} \right]^{2/3} \ . \tag{21}$$

The potential energy corresponding to Eq. (12) is

$$V = \sum_i \frac{1}{\sigma_i + 1} C_i \int \rho^{\sigma_i + 1}(\mathbf{r}) d^3r + \frac{1}{2} \int v(\mathbf{r},\mathbf{r}') \rho(\mathbf{r}) \rho(\mathbf{r}') d^3r' d^3r \ , \tag{22}$$

where $\sigma_i \geq 1$, v has the dimension of energy, and the C_i's have dimensions of energy $(fm)^{3\sigma_i}$

We now consider changing $\rho(\mathbf{r})$ to $\rho(\mathbf{r}) + \delta\rho(\mathbf{r})$. Particle conservation implies this must be done subject to

$$\int \delta\rho(\mathbf{r}) d^3r = 0 \ . \tag{23}$$

In first order, the kinetic energy changes to

$$\delta T=\frac{5}{3}C\int\rho^{2/3}(\mathbf{r})\delta\rho(\mathbf{r})d^3r\ . \tag{24}$$

The potential energy changes to

$$\delta V=\int\left[\sum_i C_i\rho^{\sigma_i}(\mathbf{r})+\int v(\mathbf{r},\mathbf{r}')\rho(\mathbf{r}')d^3r'\right]\delta\rho(\mathbf{r})d^3r\ . \tag{25}$$

Taking into account number conservation, the quantity which is to be set equal to zero is

$$\frac{h^2}{2m}\left[\frac{3}{16\pi}\right]^{2/3}\rho^{2/3}(\mathbf{r})+\sum_i C_i\rho^{\sigma_i}(\mathbf{r})+\int v(\mathbf{r},\mathbf{r}')\rho(\mathbf{r}')d^3r'-\lambda=0\ , \tag{26}$$

which is the same as Eq. (17). Thus finding a self-consistent solution is equivalent to finding an extremum in energy.

To investigate stability, we need to go to second order. From Eqs. (20) and (22), we get

$$\int d^3r[\delta\rho(\mathbf{r})]^2\left[\frac{5}{9}C\rho(\mathbf{r})^{-1/3}+\frac{1}{2}\sum_i C_i\sigma_i\rho^{\sigma_i-1}(\mathbf{r})\right]+\frac{1}{2}\int d^3r\,d^3r'v(\mathbf{r},\mathbf{r}')\delta\rho(\mathbf{r})\delta\rho(\mathbf{r}')>0\ . \tag{27}$$

This will be satisfied if, in the following eigenvalue equation

$$\left[\frac{5}{9}C\rho^{-1/3}(\mathbf{r})+\frac{1}{2}\sum C_i\sigma_i\rho^{\sigma_i-1}(\mathbf{r})\right]g(\mathbf{r})+\frac{1}{2}\int d^3r'v(\mathbf{r},\mathbf{r}')g(\mathbf{r}')=\varepsilon g(\mathbf{r})\ , \tag{28}$$

the eigenvalue ε is always greater than zero; $g(\mathbf{r})$ must satisfy $\int g(\mathbf{r})d^3r=0$ due to Eq. (23). In the Hartree-Fock case, the appearance of one or more imaginary eigenvalues in the random-phase approximation (RPA) matrix implies instability.

It is nontrivial to solve Eq. (28). Since $v(\mathbf{r},\mathbf{r}')$ is symmetric in $\mathbf{r}$ and $\mathbf{r}'$, the eigenvalues ε are all real. We have verified that, for our self-consistent static solution, the eigenvalues do have a finite, positive definite lower bound. Further, the lowest solution $g(r)$ with spherical symmetry is approximately $\alpha^3\rho(\alpha r)-\rho(r)$ with $\alpha=1+\delta\alpha$. This is strongly suggestive of monopole vibration. Notice that the eigenvalue ε has the dimension MeV fm^3. The usefulness of Eq. (28) in studying monopole vibrations in finite nuclei with diffuse surfaces is being investigated.

IV. CHOICE OF FORCE PARAMETERS

A parametrization of the type of Eq. (11) with $v(\mathbf{r},\mathbf{r}')$ given by Eq. (13) was already used in TDHF.[18] This is known as the Bonche-Koonin-Negele (BKN) force. Density distributions from self-consistent Vlasov solutions with the BKN force are shown in Fig. 1. The relationship between our parameters and the BKN parameters are $\sigma=2$, $A=\frac{3}{4}t_0$, $B=3t_3/16$; BKN choose the range parameter "a" of the Yukawa from the range of G matrix in nuclear matter; the value of V_0 is then fixed from t_1 and t_2 of a Skyrme parametrization which gives $m^*/m=1$. The nuclear matter properties with this force are $E/A=-15.77$ MeV; $k_F=1.29$ fm^{-1} and the compressibility $K=368$ MeV.

The nuclear densities $\rho(r)$ for ^{16}O and ^{40}Ca with the BKN force are quite reasonable when the ground-state problem is solved in the Hartree-Fock approximation. The densities are not as reasonable when the same problem is solved in the Vlasov prescription (Fig. 1). This is hardly surprising. Compared to classical mechanics, quantum mechanics has an inherent tendency of spreading out the surface. A mean field $A\rho(r)+B\rho^{\sigma}(r)$ produces a sharp surface in the Vlasov approximation but would give a much smoother surface in the Hartree-Fock approximation. Since we intend to use the Vlasov prescription for heavy-ion collision problems, we are constrained to change the force parameters to obtain a better fit to ground-state properties in the Vlasov approximation. The properties we are looking for are (1) diffusivity of surfaces of nuclei, (2) their binding energy, and (3) the properties of infinite nuclear matter. We notice that, for this last item, only the combination $(A+4\pi V_0a^3)$ matters, not A, V_0, and a individually. We will therefore keep B, σ, and the combination $(A+4\pi V_0a^3)$ fixed [see Eqs. (11) and (13)] but vary A and a individually to obtain better fit for finite nuclei.

We therefore vary A and a to fit binding energies and surfaces. In quantum-mechanical treatments, $\rho(r)$ goes to zero asymptotically; in the Vlasov prescription, $\rho(r)$ goes to zero identically at some value r_0. For a given "A," increasing "a" increases the value of r_0 but decreases the binding energy. In Fig. 1, we have shown that a readjustment from the original BKN parameters produces reasonable surfaces in the Vlasov prescription. The parameters we recommend are

$$\begin{aligned} &A=0\ ,\\ &B=3238.1\ \text{MeV fm}^6\ ,\\ &\sigma=2\ ,\\ &a=0.459\,79\ \text{fm}\ ,\\ &V_0=-668.65\ \text{MeV}\ . \end{aligned} \tag{29}$$

Here we have absorbed the attractive field due to the $A\rho$ term entirely into an augmented Yukawa field whose range "a" is kept unchanged from the original BKN

value. The following set of parameters, whose results are also shown in Fig. 1, gives similar results:

$$A=-300 \text{ MeV fm}^3 ,$$
$$B=3238.1 \text{ MeV fm}^6 ,$$
$$\sigma=2 , \tag{30}$$
$$a=0.8 \text{ fm} ,$$
$$V_0=-80.315 \text{ MeV} .$$

The binding energy per particle for the parameters given in Eq. (29) are 4.43 MeV for ^{4}He, 7.25 MeV for ^{16}O, and 8.22 MeV for ^{40}Ca; the same numbers using the parameters of Eq. (30) are 3.04 MeV, 5.62 MeV, and 6.76 MeV, respectively. Here, and in all the calculations of this section, we have taken into account the Coulomb repulsion for better binding energies.

Introducing Coulomb interaction in the mean-field Eq. (11), one needs to distinguish between proton and neutron densities (ρ_p and ρ_n) with $\rho=\rho_n+\rho_p$. Procedures for obtaining the self-consistent densities are basically the same as a given in Sec. II. Removing isospin degeneracy, Eq. (9) is modified as

$$f(\mathbf{r},\mathbf{p})=\frac{2}{h^3}\sum_{q=n,p}\theta[\lambda_q-U^q(\mathbf{r})-p^2/2m] .$$

Thus the self-consistent equation (17) would become

$$\left[\frac{3h^3}{8\pi}\rho_{q(\mathbf{r})}\right]^{2/3}+2m[A\rho(\mathbf{r})+B\rho^{\sigma}(\mathbf{r})] =2m[\lambda_q-U_y(\mathbf{r})-U_c(\mathbf{r})\delta_{q,p}] .$$

Here $U_c(\mathbf{r})$ is the contribution due to the Coulomb part and can be treated in the same way as U_y; ρ_p and ρ_n are coupled by the mean field. Steps (ii) and (iii) in Sec. II are performed for ρ_p with λ_p and for ρ_n with λ_n.

The choice of $\sigma=\frac{7}{6}$ in Eq. (11) produces a softer equation of state. We require our force parameters to reproduce the same binding energy per particle and saturation density for nuclear matter as in BKN. In Fig. 2, we show results obtained from the following sets of parameters:

$$A=-1936.8 \text{ MeV fm}^3 ,$$
$$B=2805.3 \text{ MeV fm}^{7/2} ,$$
$$\sigma=\tfrac{7}{6} , \tag{31}$$
$$a=0.459\,79 \text{ fm} ,$$
$$V_0=-363.04 \text{ MeV} ;$$
$$A=-1563.6 \text{ MeV fm}^3 ,$$
$$B=2805.3 \text{ MeV fm}^{7/2} ,$$
$$\sigma=\tfrac{7}{6} , \tag{32}$$
$$a=0.459\,79 \text{ fm} ,$$
$$V_0=-668.65 \text{ MeV} ;$$

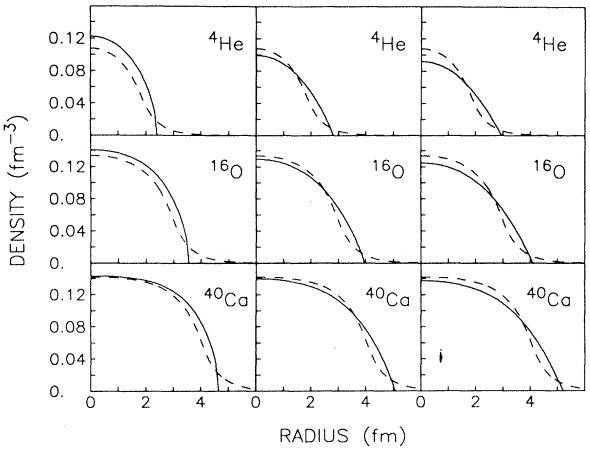

FIG. 2. Same as in Fig. 1 but with soft equation of state ($\sigma=\frac{7}{6}$). First column is with force parameter of Eq. (31), second one with Eq. (32), and the last one with Eq. (33).

$$A=-1428.2 \text{ MeV fm}^3 ,$$
$$B=2805.3 \text{ MeV fm}^{7/2} ,$$
$$\sigma=\tfrac{7}{6} , \tag{33}$$
$$a=0.459\,79 \text{ fm} ,$$
$$V_0=-779.48 \text{ MeV} .$$

The parameter set of Eq. (31) has the same Yukawa as BKN and Fig. 2 shows that this force in the classical approximation will not produce realistic diffusivity of the surface. We recommend the parameters given in Eq. (32) which has the same Yukawa as in Eq. (29). Results from the parameters set of Eq. (33) are also shown to demonstrate how small changes in the parameters set affect the binding energy and the surface. With the parameter set of Eq. (32), we obtain binding energy per particle 6.27 MeV, 8.42 MeV, and 9.08 MeV for ^{4}He, ^{16}O, and ^{40}Ca, respectively. The corresponding numbers for the parameter set of Eq. (33) are 5.63 MeV, 7.89 MeV, and 8.65 MeV, respectively.

For larger nuclei with $N\neq Z$, one may wish to fit the symmetry energy as well. Now one needs two densities ρ_p and ρ_n. Procedures for obtaining the self-consistent densities are the same as including Coulomb repulsion. However, now we have an even greater number of parameters that we can adjust to get the correct symmetry energy. We can introduce two Yukawa potentials [Eq. (13)] with strength parameters V_u and V_l, as in Ref. 19; the sum $(V_l+V_u)/2=V_0$ is already fixed from our $N=Z$ parametrization and V_l-V_u is adjusted to obtain a symmetry energy coefficient of 34 MeV. Following this prescription, we get the density distribution in ^{208}Pb (Fig. 3). For $N=Z$ systems, the force parameters used in A, B, and C (Fig. 3) become the same as used in Fig. 1; similarly, D, E, and F reduce to the force parameters used in Fig. 2. The binding energy per nucleon in ^{208}Pb varied

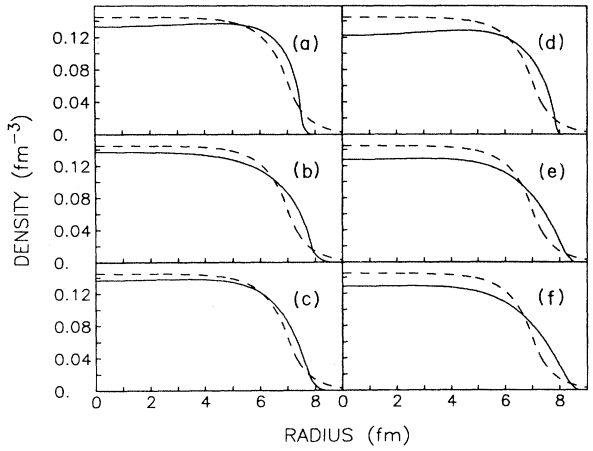

FIG. 3. Self-consistent nucleon density distributions for ^{208}Pb with symmetry energy in Yukawa potential. Left column is for stiff equation of state ($\sigma=2$) with the force parameters which become, in symmetric nucleus limit, A to BKN, B to Eq. (30), and C to Eq. (29). Right column is for soft equations of state ($\sigma=\frac{7}{6}$) with the force parameters which become, in symmetric nucleus limit, D to Eq. (31), E to Eq. (32), and F to Eq. (33).

between 6.7 and 8.9 MeV for these parameter sets. We have also tried making the zero-range terms [A and B of Eq. (11)] to distinguish between like and unlike particles keeping one Yukawa and that also works reasonably well.

One might ask why we have so many choices of parameters, whereas corresponding TDHF calculations have less freedom in the choice of parameters. In Ref. 19, the starting point is the Skyrme interaction which is a zero-range force with all fixed parameters. The Yukawa term is introduced merely as a computational convenience in order to replace the $\rho\nabla^2\rho$ term which appears in a finite system with a zero-range force. Since the coefficient of $\rho\nabla^2\rho$ was fixed, there is less freedom in the choice of the Yukawa. Our motivation is different; our forces are not entirely zero range; the Yukawa has been brought in specifically to reproduce the diffuse surface and binding energy in finite nuclei. There is some difficulty in fitting the binding energy of ^{4}He and ^{40}Ca simultaneously; but this is still an improvement. With zero-range forces in the Vlasov prescription, all finite nuclei have the same binding energy per nucleon as in nuclear matter. Thus introducing an Yukawa actually improved the fit to the binding energy in finite nuclei. We will have to reconsider the force parameters if we want to bring momentum dependence of the mean field;[6] however, our next goal will be to look at heavy-ion collisions at 50 to 100 MeV/nucleon beam energy where momentum dependence may not play a crucial role. In any case it is worthwhile to study the effect of the diffusivity without the extra complication due to momentum dependence.

V. TIME EVOLUTION

The self-consistent solutions are stationary in time. In actual collisional calculations, the time evolution is done numerically, and it is important to check if the numerical inaccuracy in time propagation will destroy the surface significantly. We use the method of test particles which has been well documented before.[20] In typical calculations a grid size of 1 fm, time step of 0.3 fm/c, and $\tilde{N}=200$ (where $\tilde{N}$ is the number of test particles per nucleon) are used. For the method of test particles to be exact, the grid size should be vanishingly small and $\tilde{N}$ infinitely large. We have mentioned that with a zero-range force the self-consistent Vlasov solution has a sharp surface. In the test particle method, which calculates the force using finite grid size, a diffuse surface will automatically develop even where, in principle, the surface is sharp. We show an example in Fig. 4 for ^{40}Ca. Here we used zero-range force but a diffuse surface develops quickly. However, the diffusivity is not enough. The oscillations in the density are due to inaccuracies in the numerical computation for time evolution. The zero-range force used in Fig. 4 gives the same properties for nuclear matter as the finite range force of Eq. (29).

In cases where the static solution has self-consistent diffuse surfaces with finite range forces, one could imagine that the accuracy of the finite grid size method will actually improve. Figure 5 shows an example, again for ^{40}Ca. We use force parameters of Eq. (29). There are significant differences between Figs. 4 and 5. Figure 5 has more realistic surface and fluctuations are not big enough to destroy the surface. A reasonable surface exists at 90 fm/c.

Compared to our previous calculations with zero-range forces, the extra work is in computing the potential $U_y(\mathbf{r})$ generated by the Yukawa;

$$U_y(\mathbf{r})=V_0\int\frac{e^{-|\mathbf{r}-\mathbf{r}'|/a}}{|\mathbf{r}-\mathbf{r}'|/a}\rho(\mathbf{r}')d^3r' .$$

This is equivalent to solving the Helmholtz equation:

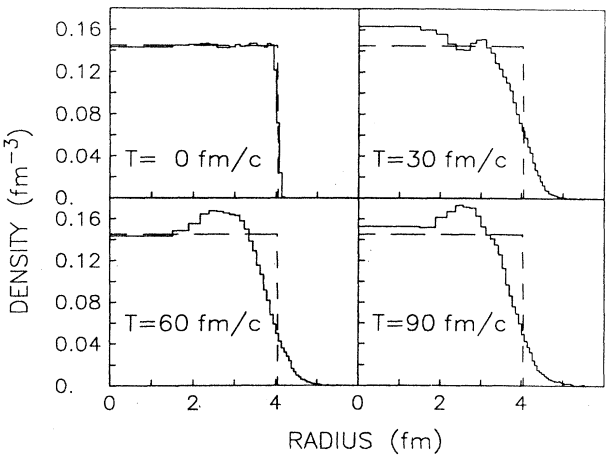

FIG. 4. Density distributions (solid line), as a function of time when the time-dependent Vlasov equation is solved by finite grid size test particle method. The force is a zero-range force and the initial density is a self-consistent Vlasov solution. In an exact calculation the density should not change.

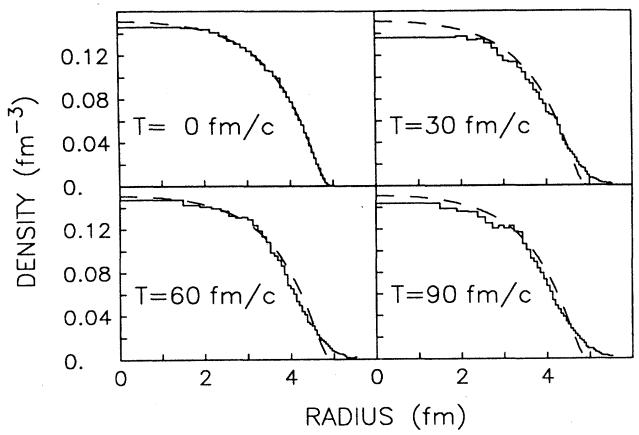

FIG. 5. Same as in Fig. 4 except that the force used is a combination of zero and finite range. Dashed line is the density distribution of the self-consistent solution.

$$\left[-\nabla^2+\frac{1}{a^2}\right]U_y(\mathbf{r})=4\pi a V_0\rho(\mathbf{r})\ .$$

Numerical solution of this equation in an axial two-dimensional grid space is standard in TDHF.[21] We have done a straightforward extension of this procedure to three dimensions. The numerical calculations shown in Fig. 5 did not exploit the spherical symmetry of the problem at hand and thus can, with equal ease, be used for collisional calculations.

In summary, the extension of the BUU model to include self-consistently calculated diffuse surfaces is straightforward and feasible. We expect to present applications of this model to specific peripheral collisions in the near future.

After this work was completed, we learned about an earlier work[22] which employed finite range forces in approximations similar to what is used in this work. This work was done in one dimension.

ACKNOWLEDGMENTS

Discussions with N. de Takacsy are gratefully acknowledged. This work was supported in part by National Science and Engineering Research Council of Canada (NSERC) and in part by the Quebec Department of Education.

[1]W. Bauer, G. F. Bertsch, and S. Das Gupta, Phys. Rev. Lett. **58**, 863 (1987).
[2]H. H. Gan, S. J. Lee, and S. Das Gupta, Phys. Rev. C **36**, 2365 (1987).
[3]G. F. Bertsch, H. Kruse, and S. Das Gupta, Phys. Rev. C **29**, 673 (1984).
[4]J. Aichelin and G. F. Bertsch, Phys. Rev. C **31**, 1730 (1985).
[5]H. Kruse, B. V. Jacak, and H. Stocker, Phys. Rev. Lett. **54**, 289 (1985).
[6]C. Gale, G. F. Bertsch, and S. Das Gupta, Phys. Rev. C **35**, 1666 (1987).
[7]H. A. Gustafsson *et al.*, Phys. Rev. Lett. **52**, 1590 (1984).
[8]K. G. R. Doss *et al.*, Phys. Rev. Lett. **57**, 302 (1986).
[9]R. Stock *et al.*, Phys. Rev. Lett. **49**, 1236 (1982).
[10]C. Gregoire, B. Remaud, F. Seville, and L. Vinet, Phys. Lett. **186**, 14 (1987).
[11]A. Bonasera, M. di Toro, and C. Gregoire, Nucl. Phys. **463**, 653 (1987).
[12]P. J. Siemens, Phys. Rev. C **1**, 98 (1970).
[13]C. Gregoire, B. Remaud, F. Sebille, L. Vinet, and Y. Raffray, Nucl. Phys. **A465**, 317 (1987).
[14]W. D. Myers, Nucl. Phys. **A296**, 177 (1978).
[15]G. Cecil, S. Das Gupta, and W. D Myers, Phys. Rev. C **22**, 2018 (1980).
[16]D. J. Thouless, Nucl. Phys. **21**, 225 (1960).
[17]D. J. Thouless, Nucl. Phys. **22**, 78 (1961).
[18]P. Bonche, S. E. Koonin, and J. W. Negele, Phys. Rev. C **13**, 1226 (1976).
[19]K. T. R. Davies and S. E. Koonin, Phys. Rev. C **23**, 2042 (1981).
[20]S. Das Gupta, C. Gale, J. Gallego, H. H. Gan, and R. D. Ratna Raju, Phys. Rev. C **35**, 556 (1987).
[21]S. E. Koonin, K. T. R. Davies, V. Maruhn-Rezwani, H. Feldmeier, S. J. Krieger, and J. W. Negele, Phys. Rev. C **15**, 1359 (1977).
[22]G. P. Maddison and D. M. Brink, Nucl. Phys. **A378**, 566 (1982).